

Spiro versus Planar Transition Structures in the Epoxidation of Simple Alkenes. A Reassessment of the Level of Theory Required

Robert D. Bach* and Olga Dmitrenko

Department of Chemistry and Biochemistry, University of Delaware, Newark, Delaware 19716

Received: February 14, 2003

High level ab initio and CASSCF calculations on the transition structure for the peroxyformic acid epoxidation of ethylene have been carried out to distinguish between a spiro versus a planar orientation of the peracid. The optimized spiro CASSCF (12,12)/6-31+G(d,p) transition structure (Figure 1a) is a first-order saddle point that is 4.0 kcal/mol lower in energy than the corresponding planar TS after correction for dynamic correlation [CASSCF(MP2)]. The planar TS is 11.5 kcal/mol higher in energy than an unsymmetrical spiro TS. A RSPT2 (6,6)//CAS(12,12)/6-31G(d) correction also favors the spiro TS by 5.3 kcal/mol. Single-point calculations on the spiro and planar CASSCF (12,12)/6-31+G(d,p) transition structures at the UB3LYP, UQCSD(T) and UBD(T) levels favor the spiro symmetrical TS by 9.0, 7.9, and 5.4 kcal/mol [6-31+G(d,p)]. The objective choice of the active space is demonstrated to be critical to the transition structure obtained.

Introduction

The transfer of oxygen atoms to carbon–carbon double bonds remains one of the most important reactions in organic chemistry.^{1,2} The mechanism of the peracid epoxidation of alkenes, a subset of this class of reactions, has been the subject of both experimental and theoretical study for many years. More than 50 years ago, Bartlett proposed^{3a} a mechanism where the terminal oxygen atom of the peroxy acid was transferred to the carbon–carbon double bond with simultaneous transfer of the proton of the peracid to the carbonyl oxygen. This was the accepted mechanism for many years and became known as the “butterfly mechanism” because of its shape. We are not aware of the actual origin of this term but it was not in the original lecture delivered at Wayne State University.^{3b} In our earlier theoretical studies, we found that the plane of the peroxyacid moiety preferred to be perpendicular to the C=C bond axis; we coined the term “spiro transition state”⁴ to describe the local tetrahedral environment about the attacking electrophilic oxygen atom. In an idealized spiro orientation, the H–O–C–C dihedral angle is 90.0°. During the past decade,⁵ we have continued to describe various aspects of the epoxidation reaction and have reported the activation energies for numerous epoxidation reactions; the spiro orientation, with symmetrically substituted alkenes, has always been of lower energy than a planar approach where the peroxyacid is parallel with the C=C bond axis ($\angle\text{H–O–C–C} = 0.0^\circ$). The preferred spiro approach is thought to be due to a small back-bonding interaction of the distal oxygen lone-pair of electrons with the C=C π^* orbital. This favorable electronic interaction is maximized with a tetrahedral array around the developing oxirane oxygen and is “turned off” in the planar transition structure. However, these energy differences have also been reported by other groups^{6–8} to be relatively small, and it has been almost universally assumed that the spiro TS is operating. Recent experimental^{9a} and theoretical^{9b} studies involving sterically encumbered alkenes also suggest that the spiro TS is favored over a planar one.

There has also been some controversy over the symmetrical versus asymmetrical approach of the peroxyacid to the C=C double bond. Second-order Moller–Plesset theory (MP2) was used initially for most ab initio calculations involving O–O bond cleavage and seemed to provide adequate energetics for such epoxidation reactions.^{5,10a} The MP2 method, however, gave an unsymmetrical structure¹¹ where the two developing C–O bonds were of unequal length (C–O = 1.805 and 2.263 Å) that was 0.2 kcal/mol lower in energy than a symmetrical spiro structure (a second-order saddle point).^{10b} More highly correlated methods (QCISD, CCSD, and CCSD(T)) however, gave very symmetrical spiro transition structures with synchronous formation of the developing C–O oxirane bonds for symmetrically substituted alkenes.^{10b} This controversy^{10,11,12} was rather short-lived since more efficient density functional calculations (DFT) came into general use and produced symmetrical spiro transition structures, and consequently, the use of MP2 theory for O–O bond cleavage reactions has been largely discontinued. Most have assumed that this problem was behind us.

A recent report by Leszczynski and co-workers has called both the preferred transition structure for peracid epoxidation and the use of DFT calculations for such reactions into question. Based upon a series of CASSCF calculations including the CASSCF(12,12)/6-311++G(d,p) level, they suggest a nearly planar orientation of the peroxyformic acid relative to the ethylene double bond (first-order saddle point). It was concluded that the electronic structure of this TS could only be described correctly by quantum-mechanical methods that are based upon multideterminantal approaches. We have reexamined this question at several levels of theory and remain convinced that the spiro orientation is in fact the preferred approach for alkene epoxidation with peracids and that the B3LYP variant of DFT calculations remain a useful and reasonably accurate method of choice for such studies.

Computational Methods

Molecular orbital calculations using density functional theory (DFT) methods^{14a}, quadratic configuration interaction restricted and unrestricted procedures [QCISD and QCISD(T)],^{14b} and

* To whom correspondence should be addressed.

Brueckner theory^{14c-e} [BD(T)] were performed with the Gaussian 98 package.¹⁵ The Becke three-parameter hybrid functional,^{16,17} combined with the Lee, Yang, and Parr (LYP) correlation functional,¹⁸ denoted B3LYP,¹⁹ was employed in the calculations. Geometries were optimized²⁰ at the B3LYP and QCISD levels using the 6-31G(d), 6-31+G(d,p), and 6-311+G-(3df,2p) basis sets (the latter was used only for the B3LYP optimizations). The CCSD(T) calculations have been performed using the ACES II program²¹ that implements the coupled-cluster and many-body-perturbation-theory methods. The CASSCF theory^{22a} was used as given in the GAMESS program.^{22b} Multireference second-order perturbation theory corrections to the CASSCF wave function were also implemented mostly with the GAMESS^{22b} program and in part (multireference RS perturbation theory, RSPT2) using the MOLPRO²³ suite of programs. The stationary points on the potential energy surfaces were characterized by calculations of vibrational frequencies at the level of theory used in the geometry optimization.

Results and Discussion

(a) CASSCF Calculations. In an earlier paper, we carried out a thorough systematic comparison of B3LYP density functional theory with higher computational methods including QCISD, CCSD, CCSD(T), and CASSCF methods.^{10b} We concluded that the preferred orientation for peracid epoxidation of symmetrically substituted alkenes was the symmetrical spiro approach ($\angle \text{H-O-C-C} = 90.0^\circ$) albeit that the potential energy surface for the approach of the peracid was soft. The choice of the active space proved to be crucial in defining the geometry of the TS for CASSCF calculations. Although a UNO analysis suggested that only four electrons and four orbitals were active, with only two virtual orbitals (4,4), we got a highly unsymmetrical TS that was similar to that obtained at the MP2 level.¹¹ Even when the space was extended to 14 electrons in 10 orbitals (14,10), reoptimization of the geometry still led to a highly unsymmetrical structure. It was only when we included in the virtual space both σ and π orbitals of the O-C-O fragment that we got a symmetrical transition structure with a CASSCF(10,10).

The present CASSCF calculations are based largely upon a set of six filled orbitals and six virtual orbitals in the active space (12,12) and are performed with the relatively flexible [6-31+G(d,p)] basis set. These orbitals were chosen by examination of the molecular orbitals derived from UHF calculations. We used the aforementioned CASSCF(10,10)/6-31G(d) geometry and orbitals as a starting point and reoptimized the TS at the CASSCF(10,10)/6-31+G(d,p) first. As the geometry optimization proceeded, several orbitals were rotated until we got what we considered to be the best choice based upon chemical intuition and our past experience with this TS.^{10b} The optimized spiro CASSCF (12,12)/6-31+G(d,p) transition structure (Figure 1a) is a first-order saddle point ($\nu_1 = 550.11 \text{ cm}^{-1}$). It includes all of the orbitals from the previous CASSCF(10,10) calculation [π orbitals of ethylene, O1-O2, and O2-C-O3; σ orbitals of O1-O2 and O1-H; and an oxygen lone pair [lp(O1)] plus their antibonding counterparts] with an addition of the bonding combination of a diffuse *s* orbital at O1 and a $\pi_{\text{C=C}}$ orbital. The most active molecular orbitals of that TS are discussed below in connection with other transition structures found while the complete set of orbitals is given in the Supporting Information, Figure S1. The orbital occupations for the 12 orbitals are 1.99, 1.97, 1.90, 1.93, 1.96, and 1.89 and 0.17, 0.09, 0.03, 0.03, 0.02, and 0.02 electrons. Excitation of 0.36 electrons into the virtual space clearly suggests that this spiro TS has some diradical

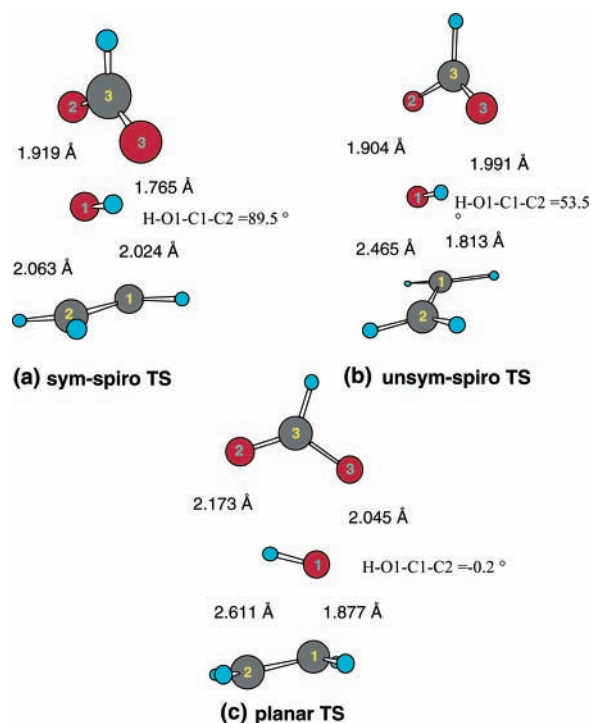


Figure 1. Three transition structures for ethylene epoxidation with peroxyformic acid optimized at the CASSCF(12,12)/6-31+G(d,p) level of theory.

character as previously noted.^{10b} The most important excitation is transfer of electron density from the ethylene π bond to the $\sigma^*_{\text{O1-O2}}$ orbital. This HOMO-LUMO interaction, based upon simple frontier molecular orbital theory, was postulated initially some 25 years ago.⁴ The TS is nearly perfectly symmetrical and spiro with an H-O-C-C dihedral angle of 89.5° , C1-O1 = 2.024 Å, C2-O1 = 2.063 Å; its overall geometry is remarkably close to that derived from QCISD, CCSD, and B3LYP calculations.^{10b}

Using a slightly modified active space (Figure 2S in the Supporting Information), we located another first-order saddle-point, spiro TS (Figure 1b, $\nu_1 = 752.31 \text{ cm}^{-1}$) but with an asymmetric approach. The TS deviates somewhat from spiro with an H-O-C-C dihedral angle of 53.5° (C1-O1 = 1.813 Å, C2-O1 = 2.466 Å). Its orbital occupations were: 1.94, 1.94, 1.87, 1.96, 1.94, and 1.72 and 0.31, 0.12, 0.10, 0.05, 0.03 and 0.02 electrons. This TS has an even more pronounced diradical character due to about one-half an electron excitation to the virtual space.

We were also able to locate a planar TS similar to the one reported by Leszczynski et al.¹³ Starting with a highly unsymmetrical spiro MP2 optimized structure^{10a,11} and using the CASSCF(6,6) approach, we located a nearly planar TS with a 6-31G* basis set using the Gaussian 98 protocol.¹⁵ The active space was expanded to (8,8), and then using GAMESS and a 6-31+G(d,p) basis set, we arrived at a CASSCF (12,12) planar TS (Figure 1c) with an H-O-C-C dihedral angle of -0.2° . The active space for this planar orientation differs from that of the symmetrical and unsymmetrical spiro TSs (Figure 3S in the Supporting Information) mainly by the absence of any contribution of an oxygen lone pair [lp(O1)]. This is in logical agreement with the suggestion that the distal oxygen lone-pair of electrons interacting with the C=C π^* orbital is the most important electronic interaction responsible for the spiro orientation. The orbital occupations are 1.98, 1.97, 1.98, 1.95, 1.87, and 1.53 and 0.53, 0.08, 0.05, 0.02, 0.03, and 0.02 electrons. Thus, the











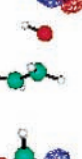


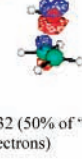
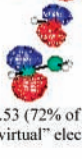
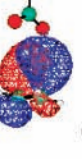



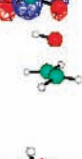
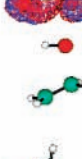

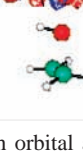

planar TS is close to becoming a diradical with 0.73 electrons in the virtual space. Lesczynski et al.¹³ also reported a high depopulation of the HOMO (0.47 e) and occupation of the LUMO (0.54 e) for this radicaloid planar transition state. We did arrive at slightly different C1–O1 and C2–O1 distances (C1–O1 = 1.877 Å, C2–O1 = 2.611 Å vs C1–O1 = 1.761 Å, C2–O1 = 2.505 Å), which could be the result of slightly different basis sets [6-31+G(d,p) versus their 6-311++G(d,p)] and active space. The single imaginary frequencies for the TSs are comparable since we observe a $\nu_i = 851.2i \text{ cm}^{-1}$ compared to their $871i \text{ cm}^{-1}$. This series of CASSCF calculations clearly demonstrate the subjective nature of choosing the active space and how relatively small changes can dramatically affect the outcome.

To get a better idea how the choice of active space affects the approach of peroxyformic acid attack on the ethylene molecule, we summarized the most active 4 occupied and 4 virtual orbitals selected from the active spaces of three CAS(12,12)/6-31+G(d,p)-optimized TSs (Table 1). The comparison of the HOMOs (antibonding combination of $\pi_{c=c}$ and σ_{O1-O2}) suggests that its occupation decreases with a decrease in symmetry, minimizing in the case of the planar TS. The next to the highest occupied molecular (HOMO–1) orbitals, (which are all bonding combinations of $\pi_{c=c}$ and σ_{O1-O2}) have almost identical occupations. The significant qualitative differences between these three TSs starts with the (HOMO–2) orbitals. In the case of the symmetrical spiro TS, (HOMO–2) is a combination of $\pi_{c=c}$ and lp(O1), whereas the unsymmetrical spiro TS has a bonding combination of $\pi_{O2-C3-O3}$ and lp(O1). In both cases, the occupation is identical, 1.93 electrons. In the planar TS, (HOMO–2) has a slightly higher occupation (1.95), and it does not contain any contribution of lp(O1); it is an antibonding combination of lp(O2) and π_{O3-C3} . Interestingly, the (HOMO–3) of the symmetrical spiro TS still has a contribution of the lp(O1) thereby providing a nearly perfect symmetrical approach. In the unsymmetrical spiro TS, (HOMO–3) is replaced by the σ orbital of the C3–O2 bond. (HOMO–3) of planar TS is σ_{O1-H} .

The two lowest virtual orbitals [LUMO and (LUMO+1)] are all of similar character (with the largest contribution from σ^*_{O1-O2}). The quantitative difference between the spiro and planar approaches becomes apparent when you analyze the distribution of electrons over the virtual space. In both spiro TSs, about 50% of electrons in the virtual space reside on the LUMO, whereas 72% of the virtual electrons belong to the lowest unoccupied orbital in the planar TS. The (LUMO+1) orbital of unsymmetrical spiro and planar TSs has the $\pi^*_{c=c}$ orbital as a major component. In the case of the symmetrical spiro TS, the combination of the lp*(O1) with $\pi^*_{c=c}$ characterizes this virtual molecular orbital (with about 25% of the overall virtual orbital electron population) thereby suggesting again the decisive role of the transferring oxygen lone-pair orbital for both symmetrical spiro approaches. Interestingly, the unsymmetrical spiro TS has the most highly occupied (LUMO+2) [$\pi^*_{O3-C3-O2}$] and (LUMO+3) [σ^*_{C3-O2}] orbitals of the three TSs. The sum of electron occupation for (LUMO+2) and (LUMO+3) is about 25% of the virtual orbital electron population, which emphasizes the importance of the virtual orbitals of the OCO moiety in stabilization of the unsymmetrical structure.

The present comparison of the MOs and their occupations given in Table 1 clearly demonstrates the necessity for at least 8 active orbitals and 8 active electrons for the location of spiro TSs. Otherwise [CAS(4,4) and CAS(6,6)], optimizations will collapse to the planar transition structures because the greatest

TABLE 1: Most Active Molecular Orbitals (from HOMO–3 to LUMO+3) Selected from the Active Spaces of Three Transition Structures for Ethylene Epoxidation with Peroxyformic Acid Optimized at the CAS(12,12)/6-31+G(d,p) Level of Theory^a

orbital	sym-spiro TS	unsym-spiro TS	planar TS
HOMO	 1.89	 1.72	 1.53
HOMO-1	 1.90	 1.87	 1.87
HOMO-2	 1.93	 1.93	 1.95
HOMO-3	 1.96	 1.94	 1.97
LUMO	 0.17 (47% of "virtual" electrons)	 0.32 (50% of "virtual" electrons)	 0.53 (72% of "virtual" electrons)
LUMO+1	 0.09	 0.12	 0.08
LUMO+2	 0.03	 0.10	 0.05
LUMO+3	 0.03	 0.05	 0.03

^a The numbers given with each orbital are corresponding electron occupations.

"orbital activity" is focused on the two highest occupied and two lowest virtual orbitals. It is essential for the spiro approach that the renowned oxygen lone-pair– π^* interaction be included in the active space.

A comparison between the total energies of the spiro and planar TSs that we have found is also informative. Indeed, the planar TS is lower in energy than both the symmetrical and

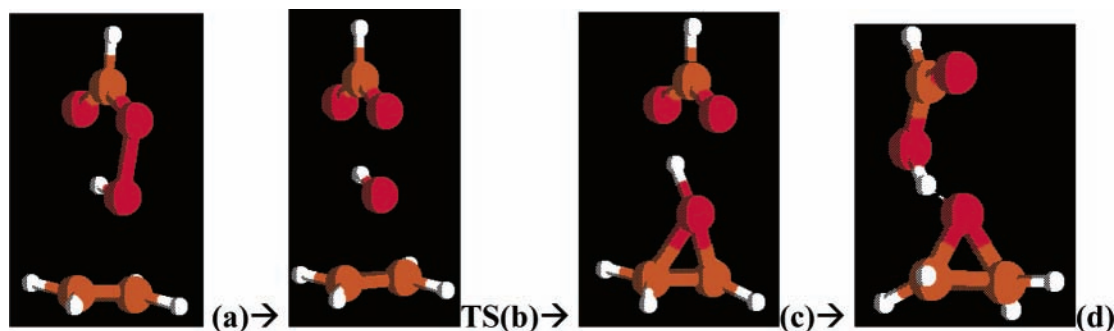


Figure 2. Selected structures from IRC calculations on the symmetrical spiro peroxyformic acid/ethylene TS at the B3LYP/6-31+G(d,p) level. Structures a and d are extreme points of the IRC calculation (reverse and forward) representing geometries close to reactant and product. Structures b and c represent the TS (saddle point of first-order) and one of the intermediate points (between the TS and an end-point structure before the 1,4-hydrogen migration to the carbonyl oxygen) of the IRC directed to the product.

TABLE 2: CASSCF(e,o)/6-31+G(d,p) Total Energies (E_{tot} , a.u.), Imaginary Frequencies (im.freq., cm^{-1}), the CASSCF(e,o)/6-31+G(d,p) Energies with MP2 Dynamic Correlation Corrections (CAS(e,o)+MP2) and Relative Energies (E_{rel} , kcal/mol) of Three Transition Structures for Ethylene Epoxidation with Peroxyformic Acid Optimized by Using Different Active Spaces^a

(e,o)	TS	E_{tot}	im.freq.	CAS(e,o)+MP2	E_{rel}
10,10	planar	-341.67508	804.9I	-342.50146	4.2
10,10	sym-spiro	-341.66296	638.7I	-342.50188	3.9
10,10	unsym-spiro	-341.65515	803.4I	-342.50813	0.0
14,11	sym-spiro	-341.64724	786.8I	-342.51743	5.8
14,11	unsym-spiro	-341.65642	779.4I	-342.52493	0.0
12,12	planar	-341.71510	851.5I	-342.50200	11.5
12,12	sym-spiro	-341.69961	550.1I	-342.50829	7.5
12,12	unsym-spiro	-341.69567	752.3I	-342.52030	0.0

^a “e” is the number of electrons and “o” is the number of orbitals in the CASSCF active space.

unsymmetrical spiro TSs by 9.7 and 12.2 kcal/mol at CASSCF(12,12)/6-31+G(d,p) [compare total energies given in Table 2, 3rd column]. However, as it is well-known, such total energies can vary markedly with the chosen active space. The planar TS is clearly a diradicaloid, and the CASSCF method tends to overemphasize the diradical character (and stabilize the planar TS). The CASSCF model is designed for recovering the effects of static correlation, whereas the MP2 method provides a low-order description of dynamical correlation.

When we correct for dynamic electron correlation with single-point CASSCF(MP2) calculations (Table 2), we find the unsymmetrical spiro TS to be 7.5 kcal/mol lower in energy than the corresponding symmetrical spiro TS, whereas the planar TS is the least stable TS in this series (11.5 kcal/mol higher than the unsymmetrical spiro TS).

CASSCF(MP2) calculations with active spaces (10,10) and (14,11) also suggest that the unsymmetrical spiro TS is the lowest-energy transition structure (Table 2). It should be noted that all of the MP2 energy corrected wave functions disfavor the planar TS. The CASPT2 calculations based upon a CASSCF(6,6) reference wave function for optimized structures at the CASSCF(12,12)/6-31G(d) level [RSPT2 correction using MOLPRO] also suggest that the symmetrical spiro orientation is favored by 5.3 kcal/mol (Table 3).

To compare the stability of all three CAS-optimized transition structures employing a common energy scale, single-point energy calculations using several single reference methods have been performed (Table 3). We have performed single point calculations on this series of TSs using UB3LYP/6-311+G(3df,2p), UBD(T)/6-311+G(d,p), and UQCISD(T)-FC/6-31+G(d,p). These relative energies provide additional data to

TABLE 3: Relative Energies (kcal/mol) of the CASSCF(12,12)-Optimized TSs for the Epoxidation of Ethylene with Peroxyformic Acid Derived from Single-Point Energy Corrections Using Different Methods^a

method	sym-spiro TS	unsym-spiro TS	planar TS
UB3LYP/6-311+G(3df,2p)	0.0	4.6	9.0
CCSD(T)/6-31G(D)	0.0		5.0
UCCSD(T)/6-31G(D)	0.0		9.0
BD(T)/6-31G(D)	0.0		6.0
BD(T)/6-311+G(d,p)	0.0	1.4	5.4
UCCSD(T)-FC/6-31+G(d,p)	0.0		8.8
RCCSD(T)-FC/6-31+G(d,p)	0.0		4.9
UQCISD(T)-FC/6-31+G(d,p)	0.0	4.4	7.9
RSPT2 (6,6)/6-31G*	0.0		5.3

^a The numbers in bold are calculated for the CASSCF(12,12)/6-31+G(d,p)-optimized TSs; plain numbers correspond to CASSCF(12,12)/6-31G(d)-optimized structures.

support the contention that the spiro approach is favored in this epoxidation reaction. With all methods, the symmetrical spiro TS exhibits the lowest total energy, whereas the planar structure is the least stable.

The peroxyformic acid/ethylene TS located with the CCSD method^{10b} also gives a symmetrical spiro structure. Geometry optimization with the triples contribution [CCSD(T)] gave a nearly identical spiro transition structure. Single-point calculations of the spiro and planar (12,12) TSs (Table 3) with the CCSD/6-31G* and UCCSD/6-31G* methods favors the spiro TS by 5.0 and 9.0 kcal/mol. With the more flexible 6-31+G(d,p) basis set, these energy differences are essentially unchanged at 4.9 and 8.8 kcal/mol (Table 3). The Brueckner doubles (BD) model is closely related to the QCISD and CCSD wave functions but differs in that the contribution of the singles excitations is eliminated and the orbitals relax in the presence of the dynamic correlation (double excitations). A BD(T)/6-31G* calculation on the (12,12) geometries suggested an energy difference of 6.0 kcal/mol (Table 3).

We also present an indirect argument for the well-accepted spiro epoxidation mechanism. Intrinsic reaction coordinate (IRC) analysis for the spiro TS (B3LYP) clearly leads to the ethylene epoxide (Figure 2). However, an IRC calculation on the CAS(6,6)/6-31G(d) planar TS (Figure 3) suggests that it does not appear to be connected directly to the ethylene oxide product. The product-like structure derived from the IRC analysis at the CAS(6,6)/6-31G(d) level is the 2-hydroxy ethyl cation H-bonded with the formate anion. This result may be due to an exaggeration of the stability of a diradical-like structure attributable to the CASSCF method. When re-optimized from the end-point of the IRC calculation, this gas phase complex is only 6.4 kcal/

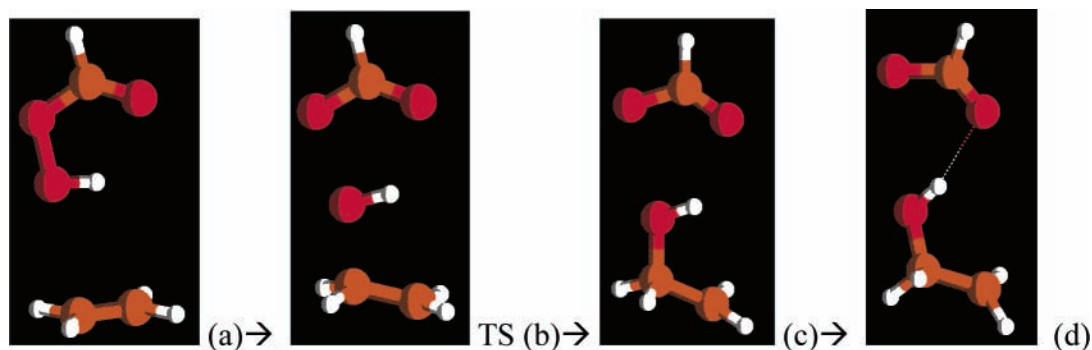


Figure 3. Selected structures from IRC calculations on the planar peroxyformic acid/ethylene TS at the *cas(6,6)/6-31G(d)* level. Structures a and c are extreme points of the IRC calculations (reverse and forward) representing geometries close to reactant and product. Structures b and d represent the TS (saddle point of first-order) and the final product (local minimum) optimized at the *cas(6,6)/6-31G(d)* level of theory.

mol lower in energy than the corresponding planar TS. The epoxidation reaction leading to ethylene oxide has an overall heat of reaction of 48.3 kcal/mol [$G_2(298.15^\circ)$].^{5c} There is no experimental evidence for the formation of a 1,2-hydroxyformate adduct under typical epoxidation conditions. Our best estimate, based upon existing information, is that the planar TS is not connected to the anticipated ethylene oxide product! Thus, we remain convinced that the spiro orientation of the peroxy acid epoxidation reaction is highly favored.

(b) QCISD Calculations. Leszczynski et al. also reported a transition structure for the peroxyformic acid/ethylene TS at the UQCISD level.¹³ Starting from the initial RQCISD symmetrical structure, they obtained a highly unsymmetrical transition state that had a spiro rather than a planar structure. This first-order saddle point had a single imaginary frequency ($\nu_i = 839i \text{ cm}^{-1}$, $C-O = 1.845$ and 2.380 \AA).¹³ However, we were puzzled by this result since we found that removal of the closed-shell restriction and reoptimization of the symmetrical RQCISD/6-31G* ethylene/peroxyformic acid TS at the unrestricted level lead to a UQCISD structure with the same geometry and total energy in a single gradient cycle. This suggests that the RQCISD solution for the spiro TS is stable; S^2 for the exact ground-state wave function is zero ($\langle S^{*2} \rangle$ is 0.0). To examine this point more closely, we took the unsymmetrical geometry reported by Leszczynski¹³ generating the force constants and initial wave functions from a single-point MP2/6-31G* (or UMP2/6-31G*) frequency calculation. In both cases, the symmetrical TS, identical to the spiro RQCISD reported by us previously,⁵ was located in about 20 and 30 gradient cycles. To re-produce the unsymmetrical UQCISD TS reported by Leszczynski et al., we performed a UQCISD reoptimization of our CASSCF(6,6)/6-31G(d) planar transition structure using force constants from a UMP2 frequency calculation and the Gaussian 98 option `guess = mix` (mixing of HOMO and LUMO). After about 50 gradient cycles, this lead to the highly unsymmetrical spiro TS that was very close to that reported in ref 13 (Cartesian coordinates and total energies are given in the Supporting Information). This structure however, has a large spin contamination ($\langle S^{*2} \rangle$ is 1.002) and its total energy is 4.3 kcal/mol higher than that of the symmetrical transition structure. The calculated activation barriers, from isolated reactants, for the RQCISD and UQCISD TSs are 25.0 and 29.3 kcal/mol. The activation barriers are significantly reduced when corrected for the triples contribution (18.8 and 25.8 kcal/mol). These data are quite consistent with our earlier suggestion that the symmetrical spiro approach is favored both on the grounds of energetics and wave function stability.^{5,10}

(c) B3LYP Calculations. Finally, because the single reference DFT method had been called into question,¹³ we reexam-

TABLE 4: Classical Activation Barriers^a (kcal/mol) for the Epoxidation of Ethylene with Peroxyformic Acid in Spiro and Planar Approaches onto the Alkene Optimized at the B3LYP/6-31+G(d,p) Level of Theory^b

alkene	$\Delta E^\ddagger(\text{spiro})$	$\Delta E^\ddagger(\text{planar})$	$\Delta\Delta E^\ddagger$
ethylene	14.9	18.6	3.7
<i>E</i> -2-butene	11.0	13.6	2.6
tetramethylethylene	7.9	9.7	1.8

^a Barriers are relative to the isolated reactants. ^b Energy differences ($\Delta\Delta E^\ddagger$, kcal/mol) between spiro and planar transition structures are given in the last column. Planar structures are optimized with fixed $\text{HOCC} = 0$ dihedral angle to produce saddle points of second order. Second imaginary frequencies (174.7i, 76.1i, and 52i cm^{-1} for ethylene, *E*-2-butene, and tetramethylethylene systems) represent a twisting vibration of the peroxyformic acid between spiro and planar positions.

ined several peroxyformic acid epoxidation transition structures with particular emphasis upon the spiro versus planar orientation at the B3LYP level. The spiro transition structures were fully optimized without constraint. The planar TSs were optimized albeit with the $C=C$ and $C=O$ bond or the $C=C$ and $O-H$ bonds constrained to a 0.0° dihedral angle. The energy differences between the ethylene, *E*-2-butene and tetramethylethylene TSs at B3LYP/6-31+G(d,p) were 3.7, 2.6, and 1.8 kcal/mol (Table 4).

These energy differences are relatively small and suggest that one should expect a lesser energy penalty for a planar-like approach as the carbon-carbon double bond becomes more highly substituted. The tetra substituted alkene has a higher HOMO and a much earlier TS (longer developing $C-O$ bond and a shorter $O-O$).^{5c} Alkenes strained by twist or π -bond torsion, such as *E*-cyclooctene, have TSs that deviate markedly ($H-O-C-C = 52^\circ$) from the idealized spiro one, have a highly asymmetric approach to the $C=C$, but yet can have a very low activation barrier ($\Delta E^\ddagger = 8.2$ kcal/mol, B3LYP/6311+G(3df,2p)//B3LYP/6-31+G(d,p)).^{5c} Thus, too much emphasis should not be placed upon the question of spiro versus planar orientations because the peracid approach can be affected by a number of geometric variables. This is especially true when more realistic substrates other than ethylene are considered. We reiterate, the PES for approach of the peracid to the $C=C$ double bond is typically quite soft.

The classical activation barriers for the spiro (first-order) and constrained-planar (second-order) TSs for the epoxidation of *E*-2-butene with peroxyformic acid only differ by 2.6 kcal/mol (Table 4, B3LYP/6-31+G(d,p)). Release of the planar constraint leads directly to the first-order spiro *E*-2-butene/peroxyformic acid TS. When the closed-shell restriction is released and both TSs are re-optimized at UB3LYP/6-31+G(d,p) they have identical total energies with the RB3LYP calculations indicating

that the restricted solution for *both* TSs is stable. The planar TS is a second-order saddle point at this level with two imaginary frequencies ($\nu_i = 3731 \text{ cm}^{-1}$ and 571 cm^{-1}). The second imaginary frequency corresponds to rotation of the peracid moiety toward a spiro orientation. However, on the B3LYP surface, where the planar TS is second-order, this TS is connected to the epoxide and the attacking oxygen is bonding to *both* alkene carbon atoms. An intrinsic reaction coordinate (IRC) analysis from the planar *E*-2-butene TS leads directly to the protonated epoxide with the proton being transferred to the formate anion along the reaction coordinate but after the barrier is crossed. Thus, a planar TS can lead to an epoxide via the intermediacy of the protonated oxirane. In contrast to the above CASSCF(6,6) IRC analysis of a planar TS, no ionic or diradicaloid 2-hydroxyethyl cationic species was located at the B3LYP level as a discrete intermediate on this reaction coordinate.

Conclusions

Contrary to the position taken by Leszczynski et al.¹³ that stated that the geometry for the planar TS “virtually does not depend on the chosen set of active space for the CASSCF approximation”, we find that the choice of active orbitals is critical. We emphasized this point in our earlier CASSCF treatment of this basic reaction.^{5b} Thus, as generally perceived, CASSCF calculations prove to be difficult and can be deceptive because the choice of active space is so subjective. Basing conclusions upon CASSCF relative total energies can also be misleading. Recovering the effects of dynamic correlation is an essential part of this exercise before their total energies can be compared. Although we concur with the Leszczynski study that the total energy of the planar peroxyformic acid/ethylene TS is lower with several different choices of active space, when corrected for dynamic electron correlation (CASSCF(MP2) or RSPT2) in each case, the spiro TS had a lower total energy. The wave functions for the spiro TS are also more stable, have less diradicaloid character, and have less electron transfer to the virtual orbitals.

All lines of evidence presented in this study, without exception, support the time-tested spiro mechanism for peracid epoxidation of ethylene and its alkyl substituted analogues. This conclusion is supported by single-point calculations on the CASSCF TSs by such single reference methods as B3LYP, QCISD (T), CCSD(T), and BD(T) methods.

A reexamination of the use of the B3LYP method for the peracid epoxidation of alkenes in conjunction with our comparative analyses of the different theoretical methods (including CASSCF) reported in ref 5c confirms our initial conclusion^{5a,b} that this density functional variant provides an adequate method for the study of such oxidation reactions involving cleavage of an O–O bond. We hope that the controversy concerning the mechanism of epoxidation and the correct theoretical method for the study of such reactions has finally been resolved satisfactorily.

Acknowledgment. This work was supported by the National Science Foundation (CHE-0138632) and by National Computational Science Alliance under CHE990021N and utilized the NCSA SGI Origin2000 and University of Kentucky HP Superdome.

Supporting Information Available: Total energies, Cartesian coordinates, and active spaces TSs optimized at the

CAS(o,e)/6-31+G(d,p) levels of theory [Figures S1–S3] with o (number of orbitals) and e (number of electrons) varying from 8 to 14, Cartesian coordinates, active spaces, and energies of the CAS(12,12)/6-31G(d)-optimized planar and spiro symmetrical TSs; single-point corrections at the different level of theories [Tables S1 and S2]. Cartesian coordinates and total energies [Table S3] of symmetrical and unsymmetrical TSs optimized at the QCISD-FC/6-31G(d) level of theory; B3LYP/6-31+G(d,p) total energies [Table S4]. This material is available free of charge via the Internet at <http://pubs.acs.org>

References and Notes

- (1) (a) Plesnicar, B. In *The Chemistry of Peroxides*; Patai, S., Ed.; John Wiley and Sons: New York, 1983; p 521. (b) Finn, M. G.; Sharpless, K. B. *Asymmetric Synth.* **1986**, *5*, 247. (c) *Organic Peroxides Vol. II*; Swern, D., Ed., Wiley-Interscience: New York, 1971; Chapter 5.
- (2) For an excellent review on substrate-directable chemical reactions, see: Hoveyda, A. H.; Evans, D. A.; Fu, G. C. *Chem. Rev.* **1993**, *93*, 1307.
- (3) (a) Bartlett, P. D. *Rec. Chem. Prog.* **1950**, *11*, 47. (b) The Frontiers in Chemistry lectures at Wayne State University, Detroit Mi, were published as a series of lectures in the Record of Chemical Progress up until 1971.
- (4) (a) Bach, R. D.; Willis, C. L.; Domagals, J. M. In *Applications of MO theory in Organic Chemistry*; Csizmadia, I. C., Ed.; Elsevier: Amsterdam, 1977; Vol. 2, p 221. (b) Lang, T. J.; Wolber, G. J.; Bach, R. D. *J. Am. Chem. Soc.* **1981**, *103*, 3275. (c) Bach, R. D.; Wolber, G. J. *J. Am. Chem. Soc.* **1984**, *106*, 1410.
- (5) (a) Bach, R. D.; Owensby, A. L.; González, C.; Schlegel, H. B.; McDouall, J. J. W. *J. Am. Chem. Soc.* **1991**, *113*, 2338. (b) Bach, R. D.; Glukhovtsev, M. N.; González, C. *J. Am. Chem. Soc.* **1998**, *120*, 9902. (c) Bach, R. D.; Dmitrenko, O.; Adam, W.; Schambony, S. *J. Am. Chem. Soc.* **2003**, *125* (4), 924.
- (6) (a) Houk, K. N.; Liu, J.; DeMello, N. C.; Condroski, K. R. *J. Am. Chem. Soc.* **1997**, *119*, 10147. (b) Houk, K. N.; Washington, I. *Angew. Chem., Int. Ed.* **2001**, *40*, 2001.
- (7) (a) Freccero, M.; Gandolfi, R.; Sarzi-Amadè, M.; Rastelli, A. *J. Org. Chem.* **1999**, *64*, 2030. (b) Freccero, M.; Gandolfi, R.; Sarzi-Amadè, M.; Rastelli, A. *J. Org. Chem.* **2000**, *65*, 8948.
- (8) Deubel, D. V. *J. Org. Chem.* **2001**, *66*, 3790.
- (9) (a) Koerner, T.; Slebocka-Tilk, H.; Brown, R. S. *J. Org. Chem.* **1999**, *64*, 4, 196. (b) Freccero, M.; Gandolfi, R.; Sarzi-Amadè, M.; Rastelli, A. *J. Org. Chem.* **2002**, *67* (24), 8519.
- (10) (a) Bach, R. D.; Winter, J. E.; McDouall, J. J. W. *J. Am. Chem. Soc.* **1995**, *117*, 8586. (b) Bach, R. D.; Glukhovtsev, M. N.; Gonzalez, C.; Marquez, M.; Estevez, C. M.; Baboul, A. G.; Schlegel, H. B. *J. Phys. Chem. A* **1997**, *101* (34), 6092.
- (11) Yamabe, S.; Kondou, C.; Minato, T. *J. Org. Chem.* **1996**, *61*, 616.
- (12) Singleton, D. A.; Merrigan, S. R.; Liu, J.; Houk, K. N. *J. Am. Chem. Soc.* **1997**, *119*, 3385.
- (13) Okovytyy, S.; Gorg, L.; Leszczynski, J. *Tetrahedron Lett.* **2002**, *43*, 4215.
- (14) (a) Hehre, W. J.; Radom, L.; Schleyer, P. v. R.; Pople, J. A. *Ab Initio Molecular Orbital Theory*; Wiley: New York, 1986. (b) Pople, J. A.; Head-Gordon, M.; Raghavachari, K. *J. Chem. Phys.* **1987**, *87*, 5968. (c) Handy, N. C.; Pople, J. A.; Head-Gordon, M.; Raghavachari, K.; Trucks, G. W. *Chem. Phys. Lett.* **1989**, *164*, 185. (d) Dykstra, C. E. *Chem. Phys. Lett.* **1977**, *45*, 466. (e) Raghavachari, K.; Pople, J. A.; Replogle, E. S.; Head-Gordon, M. *J. Phys. Chem.* **1990**, *94*, 5579.
- (15) Frisch, M. J.; Trucks, G. W.; Schlegel, H. B.; Scuseria, G. E.; Robb, M. A.; Cheeseman, J. R.; Zakrzewski, V. G.; Montgomery, J. A., Jr.; Stratmann, R. E.; Burant, J. C.; Dapprich, S.; Millam, J. M.; Daniels, A. D.; Kudin, K. N.; Strain, M. C.; Farkas, O.; Tomasi, J.; Barone, V.; Cossi, M.; Cammi, R.; Mennucci, B.; Pomelli, C.; Adamo, C.; Clifford, S.; Ochterski, J.; Petersson, G. A.; Ayala, P. Y.; Cui, Q.; Morokuma, K.; Malick, D. K.; Rabuck, A. D.; Raghavachari, K.; Foresman, J. B.; Cioslowski, J.; Ortiz, J. V.; Stefanov, B. B.; Liu, G.; Liashenko, A.; Piskorz, P.; Komaromi, I.; Gomperts, R.; Martin, R. L.; Fox, D. J.; Keith, T.; Al-Laham, M. A.; Peng, C. Y.; Nanayakkara, A.; Gonzalez, C.; Challacombe, M.; Gill, P. M. W.; Johnson, B. G.; Chen, W.; Wong, M. W.; Andres, J. L.; Head-Gordon, M.; Replogle, E. S.; Pople, J. A. *Gaussian 98*, revision A.7; Gaussian, Inc.: Pittsburgh, PA, 1998.
- (16) Becke, A. D. *Phys. Rev. A* **1988**, *38*, 3098–3100.
- (17) Becke, A. D., *J. Chem. Phys.* **1993**, *98*, 5648–5652.
- (18) Lee, C.; Yang, W.; Parr, R. G., *Phys. Rev. B* **1988**, *37*, 785–789.
- (19) Stevens, P. J.; Devlin, F. J.; Chabalowski, C. F.; Frisch, M. J. *J. Phys. Chem.* **1994**, *98*, 11623–11627.
- (20) (a) Schlegel, H. B. *J. Comput. Chem.* **1982**, *3*, 214. (b) Schlegel, H. B. *Adv. Chem. Phys.* **1987**, *67*, 249. (c) Schlegel, H. B. In *Modern Electronic Structure Theory*; Yarkony, D. R., Ed.; World Scientific: Singapore, 1995; p 459.

(21) Stanton, J. F.; Gauss, J.; Watts, J. D.; Nooijen, M.; Oliphant, N.; Perera, S. A.; Szalay, P. G.; Lauderdale, W. J.; Kucharski, S. A.; Gwaltney, S. R.; Beck, S.; Balková, A.; Bernholdt, D. E.; Baeck, K. K.; Rozyczko, P.; Sekino, H.; Hober, C.; Bartlett, R. J. *ACES II*; Quantum Theory Project, University of Florida: Gainesville, FL.

(22) (a) Hegerty, D.; Robb, M. A. *Mol. Phys.* **1979**, 38, 1795. (b) The GAMESS (General atomic and molecular electronic structure system) program: Schmidt, M. W.; Baldrige, K. K.; Boatz, J. A.; Elbert, S. T.; Gordon, M. S.; Jensen, J. H.; Koseki, S.; Matsunaga, N.; Nguyen, K. A.; Su, S.; Windus, T. L.; Dupuis, M.; Montgomery, J. A., Jr. *J. Comput. Chem.*

1993, 14, 1347. (c) Fletcher, G. D.; Schmidt, M. W.; Gordon, M. S. *Adv. Chem. Phys.* **1999**, 110, 267.

(23) MOLPRO is a package of ab initio programs designed by Werner, H.-J.; Knowles, P. J.; The authors are Amos, R. D.; Bernhardsson, A.; Berning, A.; Celani, P.; Cooper, D. L.; Deegan, M. J. O.; Dobbyn, A. J.; Eckert, F.; Hampel, C.; Hetzer, G.; Knowles, P. J.; Korona, T.; Lindh, R.; Lloyd, A. W.; McNicholas, S. J.; Manby, F. R.; Meyer, W.; Mura, M. E.; Nicklass, A.; Palmieri, P.; Pitzer, R.; Rauhut, G.; Schütz, M.; Schumann, U.; Stoll, H.; Stone, A. J.; Tarroni, R.; Thorsteinsson, T.; Werner, H.-J.